



Local metallicity in simulated galaxies

F. Collacchioni^{1,2}, C.A. Correa⁴, C.D.P. Lagos^{5,6} & S.A. Cora^{1,2}

¹ *Instituto de Astrofísica de La Plata, CONICET–UNLP, Argentina*

² *Facultad de Ciencias Astronómicas y Geofísicas, UNLP, Argentina*

³ *Institute for Theoretical Physics Amsterdam, University of Amsterdam, Países Bajos*

⁴ *International Centre for Radio Astronomy Research, University of Western Australia, Australia*

⁵ *The Cosmic Dawn Center, Niels Bohr Institute, University of Copenhagen, Dinamarca*

Contact / fcollacchioni@fcaglp.unlp.edu.ar

Resumen / En la última década, la espectroscopía de campo integrado ha expandido nuestra comprensión de la evolución química de las galaxias, dando evidencia de un gradiente radial de la metalicidad de la fase gaseosa. En este trabajo, usamos la simulación cosmológica hidrodinámica EAGLE para estudiar las propiedades localmente resueltas de las galaxias. Mostramos que la metalicidad local del gas correlaciona con la densidad superficial de masa estelar y anticorrelaciona con la acreción de gas. Los perfiles de metalicidad resueltos actúan como buenos estimadores de la acreción de gas, y pueden ser usados para entender los cambios en el enriquecimiento químico de las galaxias.

Abstract / In the last decade, integral field spectroscopy has expanded our understanding of chemical evolution of galaxies, giving evidence of a radial gradient of gas-phase metallicity. In this work, we use the state-of-art hydrodynamical simulation EAGLE to study the resolved, local properties of galaxies. We show that the local gas metallicity correlates with the stellar mass surface density and anti-correlates with the gas accretion. Resolved metallicity profiles acts as a good estimator of gas accretion, and can be used to understand the changes in the chemical enrichment of galaxies.

Keywords / methods: numerical — galaxies: evolution — galaxies: formation

1. Introduction

Our understanding of galaxy formation and evolution has considerably improved over the years thanks to advances in the technique of integral field spectroscopy (e.g. Sánchez et al., 2012; Carton et al., 2018). This has allowed the study of resolved local properties and has given insight into the origin of the integrated relations (Rosales-Ortega et al., 2012), by finding how integrated properties (e.g., stellar mass) behave in a resolved way. “Integrated properties” refers to the average of a galaxy total property measured within an specific radius, while “resolved properties” are the ones measure in star-forming regions of about $0.5''$.

An integrated property of particular interest is the gas metallicity, which correlates with the galaxy stellar mass (M_*), star formation rate (SFR) and total gas content, among other integrated properties (Mannucci et al., 2010; Zahid et al., 2014). The origin of these relations are intertwined with the analogous resolved properties, and similar or different behaviours between the resolved properties might shed light on the formation of galaxies.

Hwang et al. (2019) studied the resolved metallicity of galaxies from MaNGA (Bundy et al., 2015) and gave insight into its correlations with the accreted gas. In their work, they analyze the possibility to use the resolved metallicity as an estimator of recent gas accretion. We use a cosmological hydrodynamic simulation to further understand the resolved metallicity of galax-

ies and its relation with the accreted gas, as well as the relation with other resolved galaxy properties. Since the measurement of gas accretion is limited in observations, our results can be of great use to clarify whether the metallicity is directly linked to the accreted gas and whether it can be a good proxy as a detector of the latter.

2. Methodology

We use the reference, high volume hydrodynamical simulation from the Evolution and Assembly of GaLaxies and their Environments (EAGLE) project*, which has a volume of 100^3 cMpc^3 . The EAGLE simulations follow the evolution of dark matter and baryons, consistent with a flat Λ CDM cosmology characterised by the Planck Collaboration et al. (2014) parameters. The sub-grid physical models (such as radiative cooling, star formation, stellar feedback, etc.) are detailed in Schaye et al. (2015) and Crain et al. (2015).

In order to determine local properties, we need to identify the resolved regions of the simulated galaxies. To do so, we first rotate all galaxies setting their stellar angular momentum along the z -axis. Secondly, we apply a mesh to each galaxy, so their gas and star particles are distributed in cells (or *spaxels*) with dimensions $1 \text{ kpc} \times 1 \text{ kpc}$, a spatial size which defines what we call here “local region”. The spaxels’ scale is similar to what

*<http://icc.dur.ac.uk/Eagle/>

is found in observational works, and suitable with the standard resolution limit of the simulation (Trayford & Schaye, 2019). The particles within each spaxel will provide the information to calculate the local properties. For example, the stellar mass surface density, Σ_* , is obtained by summing the mass of all the star particles within a spaxel and dividing by the spaxels surface (i.e., 1 kpc^{-2}). The metallicity is defined as

$$Z = 12 + \log\left(\frac{1}{16} \frac{\Sigma_{\text{O}}}{\Sigma_{\text{H}}}\right), \quad (1)$$

where Σ_{O} and Σ_{H} are the oxygen and hydrogen mass surface densities, respectively.

To calculate the gas accreted mass onto galaxies, we follow the evolution of gas particles and compare their properties between two consecutive snapshots (i.e. between redshift $z = 0$ and $z = 0.1$). The gas accreted mass onto a given galaxy is formed by gas particles that fulfil the following conditions: (a) are classified as star-forming (SF) at $z = 0$; (b) are bound to the galaxy or not being bound to any structure at $z = 0.1$; and (c) are a non star-forming (NSF) particle at $z = 0.1$. In this sense, we study an smooth accretion of gas that triggers star formation (by requesting the change from NSF to SF). Finally, we calculate the gas accretion fraction in each spaxel as $f_{\text{accr}} = \Sigma_{\text{accr}}/\Sigma_{\text{gas}}$, where Σ_{accr} is the accreted gas mass surface density and Σ_{gas} is the total gas mass surface density. Notice that $f_{\text{accr}} \leq 1$.

In this work, we analyze the local properties of the stellar surface density Σ_* , metallicity Z , f_{accr} , and the projected galactocentric distance of a sample of star-forming, central galaxies, more massive than $\geq 10^{10} M_{\odot}$.

3. Results

Fig. 1 shows the median relation of the $z = 0$ gas phase metallicity as a function of Σ_* of the spaxels. This relation, known as the resolved mass-metallicity relation (rMZR), is the analogous of the global mass-metallicity relation (MZR), which is obtained by relating the integrated metallicity of the galaxy with the integrated stellar mass, M_* . We can see from the figure that spaxels with higher values of Σ_* correspond to higher values of metallicity, except for $\Sigma_* \gtrsim 3 M_{\odot} \text{ pc}^{-2}$ where the relation tends to invert this behaviour. This change of behaviour could be related to those spaxels being nearer the galaxies' centres and, thus, they might be affected by the active galactic nuclei feedback, which prevents the newly enriched gas to cool (Trayford & Schaye, 2019). The shape of the rMZR is similar to the one shown by the MZR, which could be evidence that the latter is a consequence of the former. If instead of analysing the spaxels of all galaxies, we separate the spaxels that lie in galaxies of an specific range of stellar mass (i.e., calculate the median of the rMZR only for those spaxels), we find that the trend remains, at least for spaxels of galaxies with $M_* \geq 10^{10} M_{\odot}$.

The left panel of Fig. 2 shows the metallicity of the spaxels as a function of the gas accretion fraction, f_{accr} , at $z = 0$. A clear anti-correlation can be seen, where spaxels with higher values of f_{accr} present lower values of

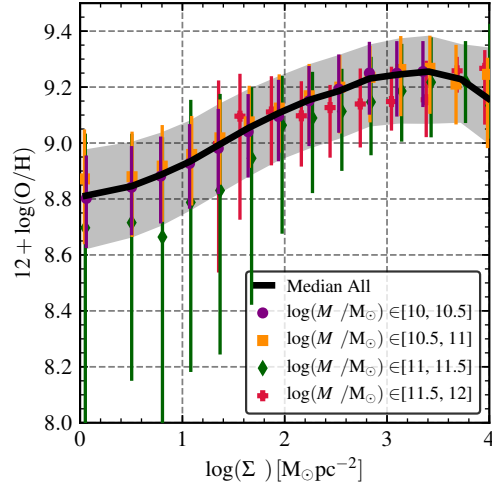


Figure 1: Metallicity of spaxels as a function of the stellar mass surface density, Σ_* , at $z = 0$. The black solid line shows the median of the relation for our simulation, while the shadows depict the 16th – 84th percentiles.

metallicity. This trend also holds for spaxels of galaxies with different stellar masses. It is worth noticing that, at fixed f_{accr} , the spaxels' metallicity increases with M_* .

To further study the $Z - f_{\text{accr}}$ anti-correlation, we define the residuals of the metallicity in the rMZR, as

$$\text{Diff}(\text{O}/\text{H}) = (\text{O}/\text{H}) - (\text{O}/\text{H})_{\text{rMZR}}, \quad (2)$$

where (O/H) is the actual value of the metallicity of the spaxel and $(\text{O}/\text{H})_{\text{rMZR}}$ is the expected value of the metallicity for the value of Σ_* of that spaxel. The right panel of Fig. 2 shows $\text{Diff}(\text{O}/\text{H})$ as a function of f_{accr} . We find that the anti-correlation remains, not only for the whole sample of spaxels but also for spaxels in specific ranges of M_* . This analysis has also been done for the $\text{Diff}(\text{O}/\text{H})$ as a function of the SFR surface density (Σ_{SFR}) in order to determine if the anti-correlation is a byproduct of the relation between other properties (not shown). To quantify the differences, we calculate the Pearson correlation coefficient (C_{P}) and find that the $\text{Diff}(\text{O}/\text{H}) - \Sigma_{\text{SFR}}$ relation has a value of $C_{\text{P}} \approx 0.09$, while the former relation ($\text{Diff}(\text{O}/\text{H}) - f_{\text{accr}}$) has a $C_{\text{P}} \approx -0.42$. This indicates that the local metallicity of galaxies is more sensitive to the local gas accretion than the Σ_{SFR} .

Fig. 3 shows the number of spaxels (represented as percentage) with different values of f_{accr} as a function of galactocentric distance at $z = 0$. We can see that spaxels with low value of f_{accr} (i.e., $\lesssim 0.5$) dominate the galaxies internal regions ($\lesssim 5 \text{ kpc}$). On the contrary, spaxels with extremely high values of f_{accr} (i.e., $\gtrsim 0.75$) dominate the external regions ($\gtrsim 10 \text{ kpc}$). This result indicates that the spaxels with higher values of f_{accr} , which are also the ones with the lower metallicity, are located in the outer regions of the galaxies. Even though there is a preference region in which spaxels of higher f_{accr} locate, the fact that these type of spaxels can be found in the inner regions ($\approx 10\%$ of $f_{\text{accr}} \geq 0.75$ and

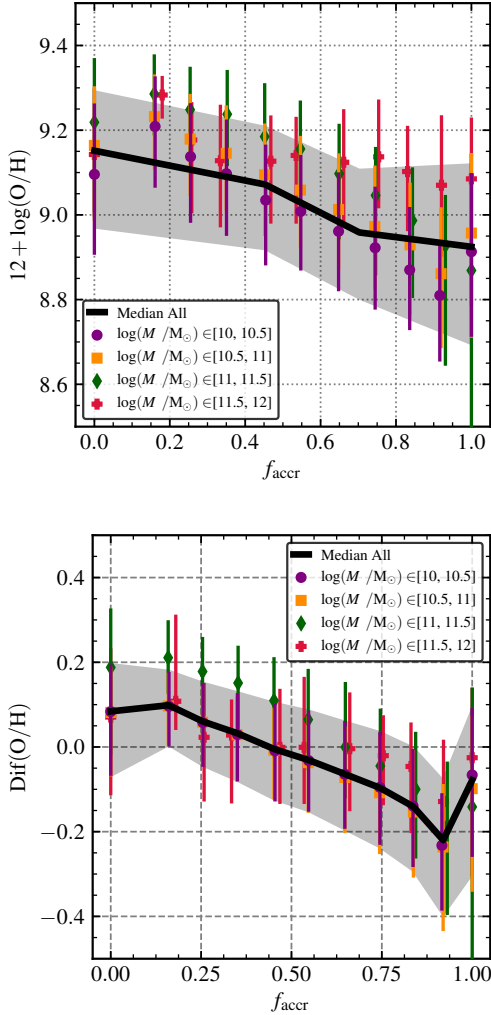


Figure 2: *Top panel:* Metallicity of the spaxels as a function of the gas accretion fraction, f_{accr} , at $z = 0$. *Bottom panel:* Residuals of the metallicity as a function of the gas accretion fraction, f_{accr} , at $z = 0$. In both panels, the black solid line shows the median of the relation for our simulation, while the shadows depict the 16th – 84th percentiles.

$\approx 30\%$ of $f_{\text{accr}} \geq 0.5$ at distances ≤ 5 kpc) tells us that the gas accretion takes place across the galaxy.

4. Conclusions

We use the EAGLE reference cosmological simulation to study how the local accretion of gas changes the metallicity of the local regions of galaxies. We investigate how the local metallicity correlates with the Σ_* , finding that it has similar trends as its integrated analogous. We study how the local metallicity relates with the f_{accr} , and find that spaxels with higher values of f_{accr} show lower values of metallicity. Measured by means of the Pearson correlation coefficient, we confirm that this anti-correlation is stronger than that obtained as a function of the Σ_{SFR} . We conclude that the metallicity is more sensitive to the f_{accr} than to other local proper-

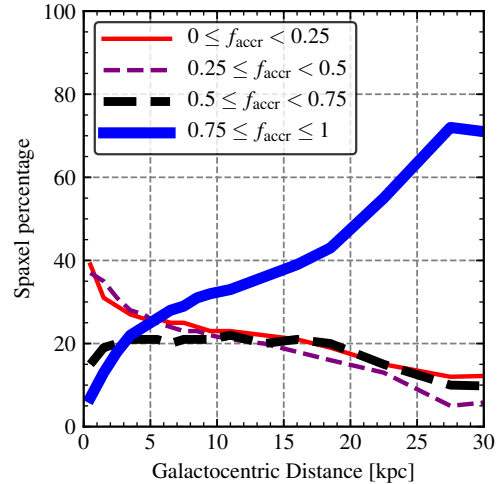


Figure 3: Number of spaxels as a function of the galactocentric distance, at $z = 0$. The spaxels are classified as the value of their gas accretion fraction, f_{accr} . Spaxels with $f_{\text{accr}} \leq 0.25$, $0.25 < f_{\text{accr}} \leq 0.5$, $0.5 < f_{\text{accr}} \leq 0.75$, and $f_{\text{accr}} \geq 0.75$ are represented by the thin solid red line, the thin dashed purple line, the thick dashed black line and the thick solid blue line, respectively.

ties. We also show the spatial distribution of the spaxels and find that, although there is accretion of gas at all radius, there is a higher amount of spaxels with higher values of f_{accr} located in the external regions.

Acknowledgements: We thank the referee for the constructive comments that improved this manuscript. We acknowledge the Local Organizer and Scientific Committees of the 62th Meeting of the AAA. We acknowledge the Virgo Consortium for making their simulation data available and the Swinburne supercomputer OzSTAR. The EAGLE simulations were performed using the DiRAC-2 facility at Durham, managed by the ICC, and the PRACE facility Curie based in France at TGCC, CEA, Bruyères-Châtel. We acknowledge funding from Consejo Nacional de Investigaciones Científicas y Técnicas (CONICET, PIP-0387), Agencia Nacional de Promoción de la Investigación, el Desarrollo Tecnológico y la Innovación (PICT-2018-3743), and Universidad Nacional de La Plata (11-G150), Argentina. This project has received funding from the European Union’s Horizon 2020 Research and Innovation Programme under the Marie Skłodowska-Curie grant agreement No 734374. FC acknowledges CONICET for its supporting fellowship. CL acknowledges the Australian Research Council Centre of Excellence for All Sky Astrophysics in 3D.

References

- Bundy K., et al., 2015, ApJ, 798, 7
- Carton D., et al., 2018, MNRAS, 478, 4293
- Crain R.A., et al., 2015, MNRAS, 450, 1937
- Hwang H.C., et al., 2019, ApJ, 872, 144
- Mannucci F., et al., 2010, MNRAS, 408, 2115
- Planck Collaboration, et al., 2014, A&A, 571, A16
- Rosales-Ortega F.F., et al., 2012, ApJL, 756, L31
- Sánchez S.F., et al., 2012, A&A, 538, A8
- Schaye J., et al., 2015, MNRAS, 446, 521
- Trayford J.W., Schaye J., 2019, MNRAS, 485, 5715
- Zahid H.J., et al., 2014, ApJ, 791, 130